Interaction of the Baculovirus Anti-apoptotic Protein p35 with Caspases. Specificity, Kinetics, and Characterization of the Caspase/p35 Complex†

Qiao Zhou,‡,§ Joseph F. Krebs,‖ Scott J. Snipas,‡ Annamarie Price,‡ Emad S. Alnemri,⊥ Kevin J. Tomaselli,‖ and Guy S. Salvesen*,‡

The Burnham Institute, Program on Apoptosis and Cell Death Research, 10901 North Torrey Pines Road, La Jolla, California 92037, Department of Pathology, Duke University Medical Center, Durham, North Carolina 27710, Idun Pharmaceuticals, 11085 North Torrey Pines Road, La Jolla, California 92037, and Center for Apoptosis Research, Kimmel Cancer Institute, Thomas Jefferson University, Philadelphia, Pennsylvania 19107

Received April 20, 1998; Revised Manuscript Received May 27, 1998

ABSTRACT: The anti-apoptotic protein p35 from baculovirus is thought to prevent the suicidal response of infected insect cells by inhibiting caspases. Ectopic expression of p35 in a number of transgenic animals or cell lines is also anti-apoptotic, giving rise to the hypothesis that the protein is a general inhibitor of caspases. We have verified this hypothesis by demonstrating that purified recombinant p35 inhibits human caspase-1, -3, -6, -7, -8, and -10 with k_{ass} values from 1.2×10^3 to 7×10^5 (M^{-1} s^{-1}), and with upper limits of K_i values from 0.1 to 9 nM. Inhibition of 12 unrelated serine or cysteine proteases was insignificant, implying that p35 is a potent caspase-specific inhibitor. Mutation of the putative inhibitory loop to favor caspase-1 resulted in a substantial decline in caspase-3 inhibition, but minimal changes in caspase-1 inhibition. The interaction of p35 with caspase-3, as a model of the inhibitory mechanism, revealed classic slow-binding inhibition, with both active-sites of the caspase-3 dimer acting equally and independently. Inhibition resulted from complex formation between the enzyme and inhibitor, which could be visualized under nondenaturing conditions, but was dissociated by SDS to give p35 cleaved at Asp87, the P_1 residue of the inhibitor. Complex formation requires the substrate-binding cleft to be unoccupied. Taken together, these data revealed that p35 is an active-site-directed inhibitor highly adapted to inhibiting caspases.

Regulation of apoptosis is vital to the development and long-term survival of metazoan animals. Apoptosis is required to maintain the balance between cell proliferation and cell death, and therefore disruptions in the apoptotic program are associated with pathologies such as cancer, where there is too little cell death, and degenerative diseases, where there is too much cell death. Apoptosis can be initiated by a variety of signals, such as specific receptor ligation, genotoxic damage, anti-cancer drugs, and delivery of specific proteases into target cells (*1*, *2*). Key mediators that initiate and execute the apoptotic program are members of the caspase family of cysteine proteases whose activation is believed to be required for apoptosis to occur in most instances (*3*−*5*). Regulation of caspases by pro- or anti-apoptotic molecules thus constitutes the major basis for precise control of apoptosis.

In humans, the 10 currently known caspases participate in one of two distinct signaling pathways: (i) activation of pro-inflammatory cytokines, (ii) promotion of apoptotic cell death. The apoptotic caspases apparently exist in a hierarchical relationship, with initiator caspases responding directly to cell death stimuli to activate distinct executioner caspases. The executioner caspases act on proteins whose cleavage is required for completion of the apoptotic program and demise of the cell (for reviews, see refs *3*, *5*). Clearly, inhibition of caspase activation and activity represents critical points where apoptosis may be regulated, as demonstrated by anti-apoptotic viral proteins. One of the most effective responses of animal cells to virus infection is activation of the apoptotic program, which the virus must evade to replicate. Consequently, some viruses have developed mechanisms to avoid apoptosis of infected cells by expressing potent caspase inhibitors. The cowpox virus protein CrmA[1] prevents apoptosis triggered by specific death receptor ligation by inhibiting the initiator caspase-8 (*6*, *7*). Significantly, CrmA has little affinity for executioner caspase-3, -6, and -7, though it strongly inhibits interleukin-1β converting enzyme (caspase-1), whose activity is responsible for generating the active cytokines interleukin-1β and

† This work was supported by NIH Grant HL51399.

* Author to whom correspondence should be addressed at The Burnham Institute, 10901 N. Torrey Pines Rd., La Jolla, CA 92037. Telephone: (619) 646-3114. Fax: (619) 646-3190. E-mail: gsalvesen@ljcrf.edu.

‡ The Burnham Institute.

§ Duke University Medical Center.

‖ Idun Pharmaceuticals.

⊥ Thomas Jefferson University.

[1] Ac, acetyl; AFC, 7-amino-4-trifluoromethylcoumarin; AMC, 7-amino-4-methylcoumarin; βNA, β-naphthylamide; CHAPS, 3-[(3-cholamidopropyl)dimethylammonio)]-1-propanesulfonic acid; CrmA, cytokine response modifier A; DTT, 1,4-dithio-DL-threitol; Hepes, 4-(2-hydroxyethyl)piperazine-1-ethanesulfonic acid; PAGE, polyacrylamide gel electrophoresis; pNA, *p*-nitroanilide; PTH, phenylthiohydantoin; RFU, relative fluorescence units; SDS, sodium dodecyl sulfate; TCA, trichloroacetic acid; Z, benzyloxycarbonyl.

S0006-2960(98)00893-9 CCC: $15.00
Published on Web 07/03/1998

interferon-γ inducing factor from their precursors (for reviews, see refs *3*, *5*).

Similarly, the p35 protein of baculovirus inhibits apoptosis in virally infected host insect cells (*8*−*10*). Moreover, ectopic expression of p35 also prevents apoptosis in *Caenorhabditis elegans*, *Drosophila melanogaster*, as well as in mammalian cells (*8*, *9*, *11*−*15*). The ability of p35 to prevent apoptosis has been attributed to direct inhibition of the caspases. So far, it has been shown that human caspase-1, -2, -3, and -4 (*16*), the *C. elegans* homologue Ced-3 (*13*), and the insect *Spodoptera frugiperda* caspase-1 (*17*) can all be potently inhibited by p35. These observations raise interesting questions about its target protease spectrum: Is p35 just an inhibitor of caspases, or is it an inhibitor with broader specificities? Does it inhibit all caspases, or does it demonstrate selectivity like CrmA? From a biologic perspective, since p35 is frequently used to demonstrate caspase involvement in apoptosis in vivo (*18*−*25*), it is important to determine whether it can inhibit other proteases implicated in cell death, such as granzymes (for a review, see ref *26*), calpains (for a review, see ref *27*), and the proteasome (*28*−*32*). These questions can be incorporated into the following hypothesis: p35 is a caspase-selective inhibitor that binds caspases tightly enough to abolish their activity in vivo.

To test this hypothesis we investigated the specificity of p35, using purified recombinant p35 and purified proteases including caspase-1, -3, -6, -7, -8, and -10, and 12 noncaspase proteases. We explored the kinetics and mechanism of caspase inhibition by p35.

MATERIALS AND METHODS

Recombinant p35. The cDNA encoding *Autographa californica* nuclear polyhedrosis virus p35 plus a C-terminal His_6 purification tag was cloned into the expression vector pET21b(+) (Novagen, Madison, WI) and expressed in *Escherichia coli* strain BL21(DE3)pLysS. Expression was induced with 1 mM isopropyl-β-D-1-thiogalactopyranoside at $A_{600} = 0.6$ for 4 h. The protein was purified by affinity chromatography using chelating Sepharose (Pharmacia, Piscataway, NJ) charged with $NiSO_4$ according to the manufacturer's instructions. Eluted p35 protein was >95% pure as judged by SDS−PAGE. Upon storage of p35 at 4 °C over a week, the inhibitory capacity declines. Therefore, all assays were conducted with material prepared within a week.

Mutagenesis of p35. A mutant of p35 in which residues 84 to 89 (DQMDGF) was replaced by LVADGA was constructed by overlap PCR mutagenesis. The two internal, partially complementary, mutagenic primers were (forward, primer-1) 5′-AGCCTTGTAGCGGATGGAGCCCACGATAGCATCAAGTATTTT-3′ and (reverse, primer-2) 5′-GTGGGCTCCATCCGCTACAAGGCTGTAATCGCGTTCTAGTTG-3′. The two flanking primers were (forward, primer-3) 5′-TAATACGACTCACTATAG-3′ and (reverse, primer-4) 5′-AAAAGCATGCCAAAAAACCCCTCAAGACCC-3′. PCR was carried out on a GeneAmp PCR System 2400 (Perkin-Elmer, Foster City, CA) with Vent polymerase (Biolab). The first round PCR generated two fragments using primer-1/primer-4 and primer-2/primer-3. PCR products were purified by agarose gel, and the two bands were excised and further purified using Wizard PCR purification kit (Promega, Madison, WI). The purified products were combined and used as the template for the second round PCR with the two flanking primers. The PCR product was purified and restricted with Nde I/Xho I, purified again, and ligated to pET23b(+) restricted with Nde I/Xho I. Competent cells of *E. coli* strain JM109 were transformed with the ligated vector. The full sequence of the insert was checked by cycle-sequencing using ABI dRhodamine Terminator Kit on an ABI 377 sequencer (PE Applied Biosystems, Foster City, CA) to verify the success of the mutagenesis and the absence of any other mutations. The expression plasmid was then subcloned into *E. coli* strain BL21(DE3)pLysS and expressed as the wild-type. The purity was similar to that of the wild-type.

Recombinant Caspases. Full length cDNAs encoding caspase-3, -6, and -7, and cDNAs encoding the catalytic chains of caspase-8 and -10 were cloned into pET23b(+), pET 21b(+), or pET15b (Novagen) and expressed in *E. coli* strain BL21(DE3)pLysS as previously described (*6*, *33*−*35*). Caspase-3, -6, and -7 contained a C-terminal His_6-tag and caspase-8 and -10 contained an N-terminal His_6-tag. All His_6-tagged proteins were purified by affinity chromatography using chelating Sepharose (Pharmacia) charged with $NiSO_4$ according to the manufacturer's instructions. All caspases had a >95% purity as judged by SDS−PAGE. Caspase-1 was from Nancy Thornberry (Merck, NJ). Active-site concentrations of the caspases were determined by titration with the irreversible caspase inhibitor Z-Val-Ala-Asp-fluoromethyl ketone (Z-VAD-FMK) (Bachem, Torrance, CA). The Michaelis constant (K_m) for the caspase substrates (see below) was determined by measuring and plotting the initial velocity, v, over an appropriate range of substrate concentration, [S] (1 μM up to 2 mM), and fitting the data directly to the Michaelis−Menten equation. The values of K_m were listed in Table 1 (see Results).

Other Proteases. Granzymes A, B, and K were provided by Dr. Chris Froelich (Northwestern University Medical School, Evanston, IL). Trypsin, chymotrypsin, papain, and subtilisin Carlsberg were purchased from Sigma (St. Louis, MO). Subtilisin was further purified by ion-exchange chromatography as described (*36*). Human neutrophil elastase and cathepsin G were purified from neutrophils as described (*37*). Porcine erythrocytes calpain I (μ-calpain) was purchased from Calbiochem (San Diego, CA). Human 20S proteasome was either a gift of Dr. Martin Rechsteiner (University of Utah, Salt Lake City, Utah) or was purchased from ICN Pharmaceuticals (Costa Mesa, CA).

Enzyme Substrates. The caspase substrate Ac-Asp-Glu-Val-Asp-*p*-nitroanilide (Ac-DEVD-pNA) was purchased from Biomol (Plymouth Meeting, PA), and Z-Asp-Glu-Val-Asp-7-amino-4-trifluoromethylcoumarin (Z-DEVD-AFC) and Z-Tyr-Val-Ala-Asp-7-amino-4-methylcoumarin (Z-YVAD-AMC) from Enzyme Systems Products (Dublin, CA); *tert*-butyloxycarbonyl-Val-Leu-Lys-pNA for papain, Z-Arg-Arg-AMC for cathepsin B, acetyl-Ala-Ala-Pro-Phe-pNA for chymotrypsin, subtilisin, and cathepsin G, benzoyl-Val-Gly-Arg-pNA for trypsin, succinyl-Ala-Ala-Val-pNA for human neutrophil elastase, tosyl-Gly-Pro-Arg-pNA for granzymes A and K, and succinyl-Ala-Ala-Pro-Asp-pNA for granzyme B were all from Sigma; succinyl-Leu-Tyr-AMC for the calpains, H-Ala-Ala-Phe-AMC for the chymotrypsin-like activity of proteasomes, *tert*-butyloxycarbonyl-Val-Leu-Arg-

AMC for the trypsin-like activity of proteasomes, and Z-Leu-Leu-Glu-β-naphthylamide (βNA) for the peptidylglutamyl-peptide hydrolyzing activity of proteasomes were purchased from Bachem (Torrance, CA).

General Reagents. All other reagents were of the highest grade from Sigma unless otherwise noted.

Spectrophotometry and Spectrofluorometry. Assays using colorimetric pNA substrates (maximal absorbance at 405 nm) are performed on a SpectraMAX 340 plate reader coupled with SOFTMAX software (Molecular Devices, Sunnyvale, CA). Assays using fluorogenic AMC substrates (excitation wavelength 380 nm and emission wavelength 460 nm) were carried out on a Perkin-Elmer LS50B luminescence spectrometer coupled with the FL WinLab softwares (Perkin-Elmer Corp., Norwalk, CT). AFC substrates were assayed at excitation wavelength 400 nm and emission wavelength 505 nm. βNA substrates were assayed using excitation wavelength 350 nm and emission wavelength 425 nm.

Enzyme Analysis. Enzyme analysis was applied as previously described (*6*). Briefly, the standard 100 μL reaction was started by adding enzyme to a mixture of substrate (final concentration 100−200 μM) and various amounts of inhibitor in buffer (50 mM Hepes, 100 mM NaCl, 0.1%(w/v) CHAPS, and 10% (w/v) sucrose, pH 7.4, as the core buffer with the following modifications for various proteases: 10 mM DTT for the caspases and papain; no DTT for the serine protease; 1 mM DTT, 2.2 mM KCl, and 0.54 mM $MgCl_2$ for proteasomes; 1 mM DTT and 1 mM $CaCl_2$ for μ-calpain. All reagents were preequilibrated at 37 °C for at least 5 min before mixing, and the caspases were preactivated for 5 min with 10 mM DTT. The lowest inhibitor concentration was at least 10-fold that of the enzyme. A control without inhibitor was used for all progress curve experiments to ensure that no substrate depletion, product inhibition, or spontaneous enzyme inactivation occurred.

Data Analysis. Kinetic data were analyzed either by linear or nonlinear regression as appropriate. The latter was performed with the aid of the computer program Kaleidagraph (Synergy Software, Reading, PA).

SDS−PAGE and Nondenaturing PAGE. A 5−15% linear acrylamide gradient PAGE with a 2-amino-2-methyl-1,3-propanediol/glycine/HCL system with or without SDS was used for resolving proteins (*38*). Samples for SDS−PAGE were boiled in SDS sample buffer containing 50 mM DTT for 5 min and then loaded onto the stacking gel. Protein gels are stained with Coomassie Blue.

N-Terminal Sequencing of Protein Samples. For N-terminal sequencing, protein samples were resolved by SDS−PAGE or nondenaturing PAGE and transferred to Immobilon-P membrane (Millipore, Bedford, MA) by electroblotting (*39*). The membrane was briefly stained with Coomassie Brilliant Blue R250, destained, and washed with water. Appropriate bands were excised and sequenced by Edman degradation on a 476A protein sequencer (Applied Biosystems, Foster City, CA).

RESULTS

Specificity of p35. As a crude initial test for inhibition, proteases (10^{-9}−10^{-8} M) were incubated with a vast excess (10^{-6} M) of p35 in an appropriate buffer for 30 min at 37 °C. An appropriate substrate was added and velocities were observed in the absence or presence of p35. Strong inhibition was detected for all caspases tested, and very weak inhibition was observed for papain, cathepsin B, cathepsin G, and the proteasome. No inhibition was detected, up to p35 concentration of 10^{-6} M, for granzymes A, B, or K, neutrophil elastase, trypsin, chymotrypsin, calpain, or subtilisin.

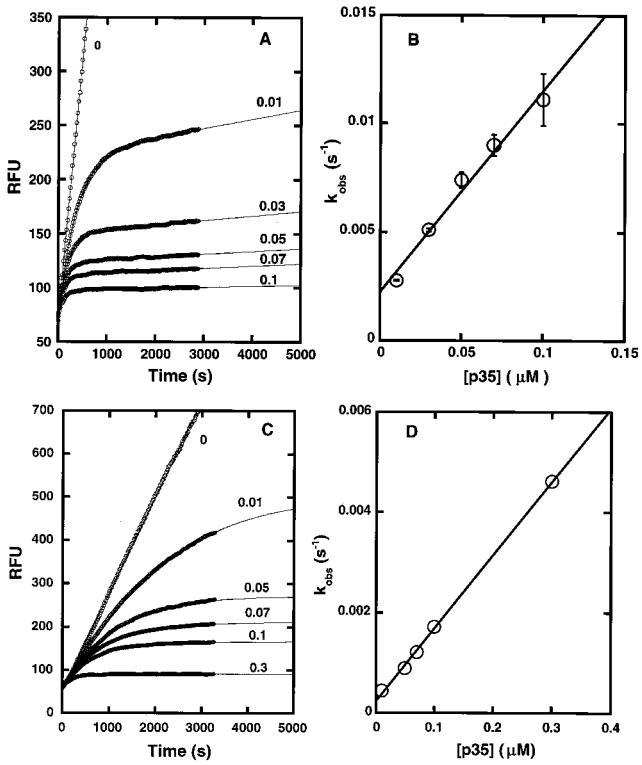

FIGURE 1: Progress curve analysis of caspase-3 (panels A and B) and 8 (panels C and D) inhibition by p35. Caspases were added to mixtures of assay buffer containing the fluorogenic substrate Z-DEVD-AFC and various amounts of p35. Substrate hydrolysis, expressed as relative fluorescence units (RFU), was determined at 10 s intervals. Final concentrations of caspase-3 and -8 were 0.1 and 1 nM, respectively. p35 concentrations (μM) were shown by numbers associated with each curve. The time-dependent loss in activity was fit to eq 1 (solid lines). The pseudo-first-order rate constant (k_{obs}) derived by the fit was plotted against [p35], the slope of which represents the second-order rate constant. Error bars are standard deviations from two or three replicated data sets. For caspase-8 (panel D), the errors were smaller than the diameter of the data symbols.

Inhibited proteases were examined in more detail by progress curve analyses. The reaction was initiated by adding enzyme to a mixture of inhibitor and substrate. Hydrolysis was recorded continuously for an appropriate period of time. Under the experimental conditions, inhibition of all the caspases demonstrated time-dependence, while the apparent weak inhibition of papain, cathepsin B, cathepsin G, and the trypsin-like and peptidylglutamyl hydrolyzing activities of the proteasome did not. Typical sets of progress curves for inhibition of caspase-8 and -3 by various concentrations of p35 are shown in Figure 1. It was not possible to further characterize the inhibition observed with papain, cathepsin B, cathepsin G, and the trypsin-like and peptidylglutamyl hydrolyzing activities of the proteasome because it was too weak (apparent $K_i > 2 \times 10^{-6}$ M). This weak inhibition seems unlikely to be of physiologic importance, and mechanistically indistinguishable from p35 acting as a competing substrate of these proteases. Indeed p35 is extensively hydrolyzed by these proteases under the experimental conditions (data not shown).

Table 1: Specificity of p35[a]

	K_m (M)	K_i (M)—upper limit	k_{ass} (M^{-1} s^{-1})
caspase-1	$1.1(\pm0.1) \times 10^{-5}$	$9.0(\pm2.9) \times 10^{-9}$	$8.2(\pm1.1) \times 10^{3}$
caspase-3	$2.4(\pm0.2) \times 10^{-5}$	$1.1(\pm0.2) \times 10^{-10}$	$7.0(\pm0.7) \times 10^{5}$
caspase-6	$1.3(\pm0.1) \times 10^{-4}$	$3.8(\pm0.6) \times 10^{-10}$	$1.3(\pm0.2) \times 10^{5}$
caspase-7	$7.7(\pm0.5) \times 10^{-5}$	$1.8(\pm0.5) \times 10^{-9}$	$1.4(\pm0.2) \times 10^{5}$
caspase-8	$2.8(\pm0.2) \times 10^{-5}$	$4.8(\pm0.9) \times 10^{-10}$	$6.4(\pm0.1) \times 10^{4}$
caspase-10	$3.9(\pm0.4) \times 10^{-4}$	$7.0(\pm1.9) \times 10^{-9}$	$1.2(\pm0.4) \times 10^{3}$

[a] Kinetic parameters [mean ± standard error of mean of two (for caspase-1 and -10) or three (for the other caspases) replicate data sets] governing the inhibition of several caspases by p35 were determined as described in the text. Calculations are based on p35 concentration derived from absorbance at 280 nM. The K_m values (mean ± standard error of mean of duplicated data sets) of the fluorogenic substrates of caspases (see Methods) are also listed.

Time-Dependent Inhibition of the Caspases by p35. The inhibition of the caspases by p35 was investigated using the progress curve method. Caspase concentrations ranged from 0.1 to 10 nM, and the p35 concentration was at least 10-fold that of the caspases. The progress curves (Figure 1) showed that p35 was not a rapid-equilibrating inhibitor of the caspases, but demonstrated features of slow-binding inhibition (*40*), similar to what had been observed with inhibition of caspases by the poxvirus serpin CrmA (*6*). The observed first-order rate constant, k_{obs}, was calculated by

$$P = v_s t - (v_s - v_0)(1 - e^{-k_{obs}t})/k_{obs} \quad (1)$$

where P is the product concentration at time t, v_0 is the initial rate of substrate hydrolysis, v_s is the final steady-state rate of substrate hydrolysis for a reversible process and would be zero for an irreversible inactivator (*40*). The parameters v_0, v_s, and k_{obs} at each p35 concentration were directly obtained by fitting the progress curve data to eq 1 (Figure 1A,C).

Plots of k_{obs} against [p35] were linear with all caspases (see Figure 1B,D for examples). The initial velocity, v_0, did not show significant change correlated to [p35]. Thus, under the experimental conditions the reactions can be described by a simple one-step model with governing rate constant k_{ass}, and overall equilibrium constant K_i. The overall inhibition constant, K_i, was calculated from the relationships $v_0/v_s = 1 + I/K_{i(app)}$ and $K_i = K_{i(app)}/(1 + [S]/K_m)$, where v_0 and v_s are defined as for eq 1, [S] is the substrate concentration, and K_m the Michaelis constant. The second-order rate constant for association, k_{ass}, was given by the slope of the k_{obs}/[p35] plot (Figure 1B,D), corrected for substrate competition by the factor $(1 + [S]/K_m)$. These inhibition parameters are tabulated in Table 1, which demonstrates that p35 is a potent inhibitor of all the caspases tested, with estimated upper limits of K_i ranging from 1.1×10^{-10} to 9×10^{-9} M, and association rates constants ranging from 1.2×10^3 to 7.0×10^5 M^{-1} s^{-1}. The K_i values should be considered as upper limits since the sensitivity of the assay precluded us from working at relatively low inhibitor concentrations around K_i. The true values of K_i may in reality be much lower than the estimates, and reversibility is thus difficult to demonstrate.

Under favorable conditions, the intercept on the *Y*-axis normally describes the dissociation rate (k_{diss}). However, this can be unreliable, and when k_{diss} is small, its magnitude is more accurately determined by direct methods. The estimated value of k_{diss} according to $K_i = k_{diss}/k_{ass}$ would be less than 10^{-5} s^{-1}. Direct measurements of k_{diss} were attempted by analyzing whether preformed enzyme−inhibitor complexes could dissociate, as follows. Caspase-3 or -6 (2.2×10^{-8} M) was incubated with equimolar p35 for 60 min at 37 °C. These conditions are more than adequate for the inhibition to proceed to near completion. Upon 500-fold (for caspase-6) or 1000-fold (for caspase-3) dilution of the reaction mixture into buffer containing a large excess of the monitoring substrate Z-DEVD-AFC, no recovery of activity above background was observed in 3 h. If an activity recovery of 10% above the background can be observed in 3 h, the half-life would be in excess of 20 h, corresponding to a dissociation rate constant of $< 1 \times 10^{-5}$ s^{-1}. This is consistent with the magnitude of the k_{diss} values estimated above, but beyond a reasonable time period for an accurate measurement.

Stoichiometry of Inhibition. The foregoing kinetic analyses are based on the assumption that inhibition obeys a simple bimolecular process, and that one molecule of p35 inhibits one molecule of caspase. In this context the molecule of caspase-3 is defined as one large subunit and one small subunit, containing one active-site. The crystal structure of caspase-3 reveals two monomers arranged with inverse symmetry (*41*, *42*), and the consequences of this structure for the stoichiometry of p35 inhibition are discussed later. Since all the assays were carried out under pseudo-first-order conditions, the kinetic values depend on an accurate determination of p35 concentration. As no substrate-like burst titrant for caspases is available, we searched for a nonselective and potent affinity label that could be used to determine the active-site concentrations. A survey of potential caspase titrants revealed that Z-VAD-FMK should be useful due to its relative potency and nonselectivity (k_{ass} for the caspases around 10^4 M^{-1} s^{-1}, data not shown). This enabled us to determine the active-site concentrations of capases, analogous to the method of using L-*trans*-epoxysuccinyl-leucylamido-(4-guanidino)butane as a titrant of cysteine proteases of the papain family (*44*). The calculated extinction coefficient of p35 ($\epsilon_{280} = 40\,800$ M^{-1} cm^{-1}) was used for determining the protein concentration from absorbance at 280 nm, and on this basis the apparent stoichiometry of inhibition ranged from 1.0 for caspase-1, -6, and -8, 1.1 for caspase-10, 1.2 for caspase-7, to 1.3 for caspase-3. Data for caspase-3 are shown in Figure 2.

Characterization of the p35−Caspase Complex. Protease inhibitors usually operate by forming complexes with their targets. Having probed the inhibition mechanism and the stoichiometry of p35−caspase interaction, we then asked if the existence of such a complex could be directly demonstrated. We used caspase-3 to study the characteristics of complex formation between caspases and p35. A fixed amount of p35 was titrated with caspase-3, allowing 30 min for inhibition at 37 °C, after which samples were split for analysis by native (nondenaturing) and SDS−PAGE. Figure 3 demonstrates that complexes form between p35 and caspase-3 which are dissociated by boiling in SDS/DTT for 5 min.

When the p35 amount was fixed and the relative concentration of caspase-3 was increased, the cleavage of p35 increased in parallel to yield a characteristic p25 fragment on SDS−PAGE (Figure 3, panel B). This continued until all the p35 was exhausted, coinciding with appearance of

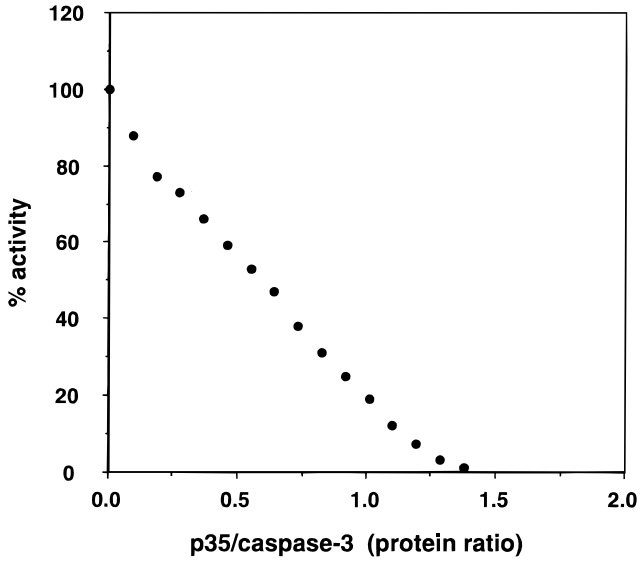

FIGURE 2: Titration of caspase-3 by p35. The active-site concentration of caspase-3 was determined by titration with Z-VAD-FMK, and then was used to determine the inhibitory concentration of freshly isolated p35. Reactants were incubated for 30 min at 37 °C, after which Ac-DEVD-pNA was added to determine residual caspase activity. The titration point corresponds to 1.3 p35 molecules per caspase-3 active-site.

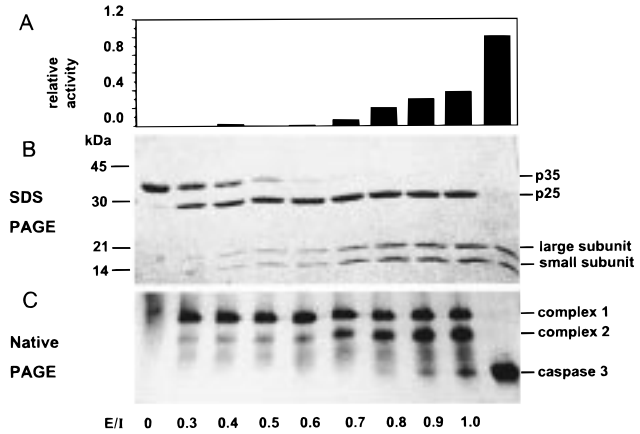

FIGURE 3: Complex formation between p35 and caspase-3. Reactions (80 μL final volume) containing 5.5 μM p35 and a range of caspase-3 from 0 to 5.5 μM were incubated at 37 °C. After 30 min, samples were withdrawn for analysis of residual caspase activity (panel A), SDS−PAGE (panel B), and native PAGE (panel C). Caspase activity is expressed relative to the maximum concentration (5.5 μM). The first lane in each gel is p35 alone, and the last lane is caspase-3 alone.

caspase activity and full cleavage of p35 at an enzyme/p35 ratio of 0.7, giving essentially the inverse ratio as when enzyme was fixed and p35 varied (see Figure 2).

In native PAGE p35 appeared as an ill-defined smear of very low mobility (Figure 3, panel C). When incubated with sub-saturating amounts of caspase-3, a more condensed band (complex 1) with higher mobility was observed. Upon saturation of p35 by caspase-3 another band with even higher mobility appears (complex 2). The identities of the two complex bands were confirmed by both N-terminal sequencing (Table 2) and 2D gels (Figure 4). The possibility that the shifted bands were cleaved p35 was excluded as each of these band contained both p35 and caspase-3. Thus, the band shift represented the formation of a complex, which was, however, dissociated by SDS. Since the gel was run under

Table 2: Amino Acid Yields of the Isolated p35/Caspase-3 Complexes[a]

	cycle	1	2	**3**	4	5	6	**7**
		Complex 1						
caspase-3	residue	S	G	**I**	S	L	D	**N**
large subunit	yield (pmol)	18.2	22.5	**15.2**	6.6	14.3	30.5	**10.6**
caspase-3	residue	S	G	**V**	D	D	D	**M**
small subunit	yield (pmol)	18.2	22.5	**12.6**	34.2	26.4	30.5	**6.7**
p35	residue	G	F	**H**	D	S	I	**K**
(p25 fragment)	yield (pmol)	15.1	16.7	**12**	34.2	17.9	7.9	**9**
		Complex 2						
caspase-3	residue	S	G	**I**	S	L	D	**N**
large subunit	yield (pmol)	40.4	71.7	**37.2**	22.7	33.6	105	**39.6**
caspase-3	residue	S	G	**V**	D	D	D	**M**
small subunit	yield (pmol)	40.4	71.7	**49.5**	81.5	68.6	105	**34.6**
p35	residue	G	F	**H**	D	S	I	**K**
(p25 fragment)	yield (pmol)	23.2	22	**17.5**	81.5	16	16.1	**18.2**

[a] Complexes 1 and 2 were isolated by nondenaturing PAGE followed by transfer to polyvinylidene difluoride membrane. Ten cycles of Edman degradation were performed and the yield of PTH amino acids in the first seven cycles (raw counts) tabulated. Because of overlaps in the residues and the frequency of unstable PTH adducts of Ser, it is difficult to compare many cycle yields of the three sequences. However, comparison of cycles 3 and 7 (in bold) is the most informative since the three sequence specific residues form relatively stable PTH adducts. Here it can be seen that the ratio of the sequence is close to unity for complex 1, and closer to 2:1 (caspase-3−p35) for complex 2.

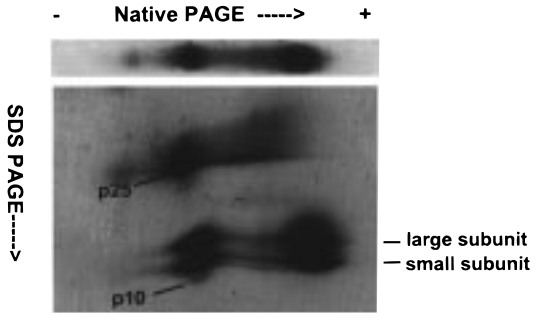

FIGURE 4: Two-dimensional PAGE analysis of complex 2. A sample of 5 μM caspase-3 was incubated with a sub-saturating quantity of p35 in 200 μL for 60 min at 37 °C. The sample was split, and half was loaded onto each of two wells in a native PAGE gel. Following electrophoresis both lanes were excised; one was stained (top of figure) and one lane was soaked for 30 min at 37 °C in SDS−PAGE sample buffer with DTT, and placed along the top of an SDS gel. Electrophoresis and staining of the SDS gel were performed as normal. In the top panel, the band on the left represents p35/caspase-3 equivalent to complex 2 (Figure 3), and the band on the right represents caspase-3.

nondenaturing conditions, the major determinants for the mobility shift are the molecular mass, the net charge, and the conformation of the molecule.

On the basis of quantitative Edman degradation, it is evident that each of the two complex bands (Figure 3, panel C) consists of both caspase-3 large and small subunits and cleaved p35. However, the composition of the two complexes was different, with a 2:1 molar ratio of caspase-3−p35 favored at high caspase concentration. A very low yield corresponding to the N-terminal p10 fragment of p35 was detected in both complexes. Either only a small amount of this fragment is associated with the complex, or, because the N-terminus of p35 is largely blocked during expression in *E. coli* (not shown), its presence is not fully visible to Edman degradation.

The composition of complex 2 as identified by two-dimensional PAGE analysis was shown in Figure 4. When

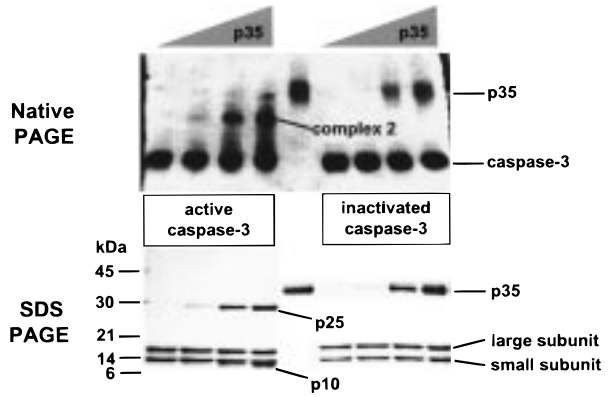

FIGURE 5: An unblocked catalytic site in caspase-3 is required for complex formation with p35. Samples of 5 μM caspase-3 or caspase-3 pretreated with 100 μM Z-DEVD-FMK were incubated with 0, 1, 2, or 3 μM p35 for 60 min at 37 °C. The samples were divided and analyzed by native PAGE (top gel) or boiled for 5 min in SDS sample buffer followed by SDS−PAGE (bottom gel). The complex seen in the native gel corresponds to the position of complex 2 (see Figure 3).

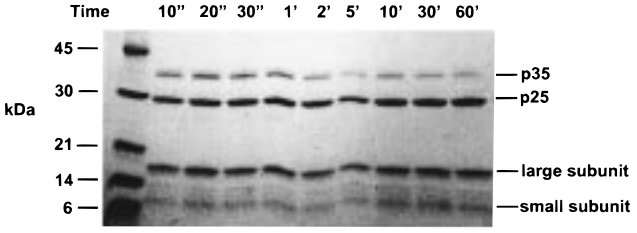

FIGURE 6: Time-dependence of p35 cleavage following reaction with caspase-3. A sample of 7 μM p35 in 350 μL was pre-warmed to 37 °C and mixed rapidly with 150 μL of 11 μM pre-warmed caspase-3. These amounts were chosen to allow 90% saturation of the inhibitory capacity of p35. At the given times, 40 μL portions were added to 20 μL of 30% TCA to terminate the reaction, samples were precipitated, washed twice with acetone/ethanol (1:1 by volume), air-dried, redissolved in 1× sample buffer, and run in SDS−PAGE.

the complex in the first-dimension native PAGE was resolved in a second-dimension SDS−PAGE, four components were identified: the large and small subunits of caspase-3, the N-terminal p10 fragment, and the C-terminal p25 fragment of p35 resulting from cleavage at Asp87.

Formation of the Complex Requires an Unblocked Active-Site. To test whether p35 is active-site directed and complex formation requires an intact active-site, p35 was incubated with either active caspase-3 or caspase-3 that had been inactivated by Z-VAD-FMK (Figure 5). Clearly, the ability to form a complex with p35 was abolished when the active-site was blocked by the irreversible peptide inhibitor.

The Rate of p35 Cleavage. Since p35 had previously been reported to be cleaved at Asp87 during its reaction with caspases (*13*, *16*, *43*) (see Table 2), we attempted to analyze how fast this occurs. To do this we mixed caspase-3 with a slight inhibitory excess of p35 and withdrew samples into 30% trichloroacetic acid (TCA) to terminate the reaction as quickly as possible (*36*). As shown in Figure 6, the cleavage was essentially complete in the first 10 s, and no additional cleavage occurred up to 60 min. Thus, irrespective of the nature of the cleavage, its half-time is much less than 10 s, corresponding to a rate constant $\gg 0.07\ s^{-1}$. These data are consistent with a requirement for specific cleavage of p35 in the inhibitory loop to establish the inhibitory complex, though we cannot rule out that the observed cleavage simply accompanies denaturation of the complex, as discussed later.

Table 3: Altered Selectivity of the p35 Loop Mutant[a]

	k_{ass} ratio (mut/wt)
caspase-1	2.9
caspase-3	**0.0125**
caspase-6	2.1
caspase-7	0.48
caspase-8	1.9
caspase-10	1.4

[a] Kinetic parameters governing the inhibition of caspases by the p35 loop mutant were determined as described for wild-type p35. Calculations are based on protein concentration calculated from absorbance at 280 nM. Ratios in the table are the kinetic values for mutant p35 divided by the respective values of the wild-type.

Inhibitory Activity of a Loop Mutant of p35. A mutant of p35 was constructed in which the P_4-P_2' residues (DQMDGF, residues 84−89) were replaced by LVADGA to simulate the CrmA reactive-site loop. This mutant was used to examine the structure−function relationship of the putative inhibitory loop of p35 and the hypothesis that the sequence of the loop will dictate its affinity for proteases. This loop sequence in the frame of CrmA is an excellent inhibitor of caspase-1 and -8 and granzyme B, but a much weaker inhibitor of caspase-3. We asked if the replacement could change the specificity of p35 so that it would become more similar to CrmA.

The apparent stoichiometry of inhibition of the mutant p35 with the caspases did not change significantly, ranging from 1.0 for caspase-1, -6, and -8, and 1.2 for caspase-3, 1.5 for caspase-7, and 1.25 for caspase-10. Inhibition of the caspases was investigated by progress curve analysis as with the wild-type. The inhibition parameters as compared to that of the wild-type are detailed in Table 3. The overall effect of the replacement is not dramatic. The loop mutant is slightly better than the wild-type for caspase-1, -6, -8, and -10, and slightly worse for caspase-7. The most obvious change is with caspase-3: a 20-fold increase in K_i and an 80-fold decrease in k_{ass}. This is probably the result of the distinct preference for Asp at the S_4 pocket of caspase-3. No inhibition of granzyme B was detected by either wild-type or mutant p35, but whereas wild-type p35 does not react with granzyme B, the mutant is now a substrate being cleaved in the inhibitory loop (data not shown).

DISCUSSION

p35 Is a Strong, Caspase-Specific Inhibitor. The baculovirus protein p35 has previously been reported to inhibit caspase-1, -2, -3, and -4 (*16*, *43*), *C. elegans* CED-3 (*13*), and *S. frugiperda* caspase-1 (*17*). In the present study, we demonstrated that it also strongly inhibits caspase-6, -7, -8, and -10. In addition, with all the other non-caspase proteases we examined, either no inhibition is observed, or the inhibition is so weak we could not characterize it, and doubtful to be of any physiological significance. Although it cannot be ruled out that other untested proteases may be inhibited by this protein, in the absence of evidence to that effect, it can be proposed that the p35 scaffold is well adapted to specifically inhibit the caspases. Thus, our results substantiate the widely held, but previously unvalidated, belief that p35 is highly specific for members of the caspase

family, but shows little ability to discriminate between individual caspases.

Inhibition Mechanism. The kinetics and mechanism for the strong and specific inhibition of the caspases by p35 has not been investigated before. By employing progress curve analysis, we demonstrated that the time-course of p35−caspase interaction is characteristic of slow-binding inhibition, in which the equilibrium among the free and bound species of enzyme and inhibitor is reached at a steady-state time scale (namely, seconds to minutes) (*40*).

Most cases of slow-binding inhibition reported so far manifested a two-step process where a rapid, usually diffusion-limited, formation of an encounter complex EI is followed by a slower isomerization to a tight EI* complex (*40*). However, our data are more consistent with a one-step mechanism, although this seems unlikely, given the experimental evidence that a cleavage step seemed to occur during inhibition (*13*, *16*, *43*), and the second-order rate constants are also 2 to 3 orders of magnitude lower than a typical, largely diffusion-controlled, bimolecular process, suggesting the existence of more than one step (*40*). More likely, the reaction follows a two-step mechanism, but we were not able to saturate the first step and, in this case, it is not possible to differentiate it from a single-step mechanism kinetically. This explanation appeared to be quite plausible, since the highest p35 concentrations we can achieve in these assays fall within the submicromolar range. p35 became insoluble at higher concentrations, preventing us from extending the inhibitor concentration to higher levels. In addition, the pseudo-first-order rate constant would be too high to be accurately measured under steady-state conditions. These issues should be addressed by further transient-state kinetic studies.

The Nature of the p35−Caspase Complex. As shown in the results, the titration points for the caspases tested are very close to 1, with the highest being 1.3 for caspase-3. We cannot rule out that this slight departure from unity is due to error in the titrations. However, it is possible that there is a small amount of partitioning with caspase-3 and -7, when some inhibitor molecules are turned over through a substrate pathway, as seen with some serpins (*45*, *46*). Nonetheless, this departure is small and hence does not significantly influence the calculation of the inhibition parameters.

Two different complexes of p35 with caspase-3 were detected. Neither was stable to SDS, and could be visualized only under nondenaturing conditions. Significantly, the composition of the complex depends on the initial molar ratio of p35 and caspase-3 in the reaction mixture, changing from an equimolar complex in p35 excess to a 2:1 molar ratio of caspase-3 to p35 when caspase-3 was in excess. This finding can be explained if caspase-3 exists as a dimer with two active-sites, as seen in 3-dimensional structure studies (*41*, *42*). Thus, when p35 is in excess, both active-sites would be occupied by p35. When caspase-3 is in excess, one p35 molecule per caspase-3 dimer would be favored, with one active-site occupied by p35 and the other free.

When [p35] vs the caspase-3 active-site concentration is close to unity, both forms of complex were observed. Assuming that the two active-sites are independent, there will be an equal chance for forming complex 1 or 2. In Figure 3, the two complexes approached similar intensities as the ratio of caspase-3 and p35 reached the titration point (see lanes where *E*/*I* were 0.7 and 0.8). Over this point, the intensity of complex 2 became slightly higher than that of complex 1, due to the actual slight excess of caspase-3 (see discussions above about stoichiometry). These observations were consistent with the hypothesis that the two active-sites are independent. This hypothesis would also predict that complex 2, with one active-site occupied by p35 and the other active-site intact, still possess enzyme activity. Evidence for this can be discerned from the data in Figure 3. The last two lanes contained equal amounts of caspase-3. The slight amount of free caspase-3 in the lane with the nominal *E*/*I* ratio = 1 is less than 1/5 of the amount in the enzyme-only lane, yet the residual activity is about 40% of the uninhibited enzyme. This can be explained if complex 2 is partially active because one of the two active-sites was unoccupied. Thus, these data are in accordance with the notion that the active species of caspase-3 is predominantly a dimer with two equal and independent active-sites. These results extend analogous observations which indicated that caspase-1 can bind independently to p35 and a biotinylated active-site-directed ligand (*16*).

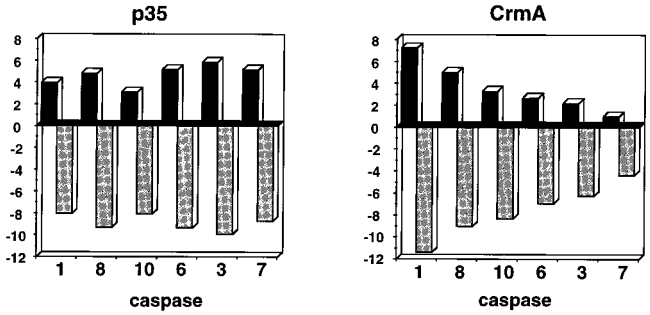

FIGURE 7: Affinities of caspases for CrmA and p35. The affinity constants are described as log K_i (grey bars), and the second-order inactivation rate constants are described as log k_{ass} (black bars), with the longest columns being the tightest or fastest inhibitors. Data for CrmA come from previous publications (*6*, *46*), with the exception of caspase-10 which was determined in this work ($k_{ass} = 1.9(\pm 0.4) \times 10^3\ M^{-1}\ s^{-1}$, $K_i = 4.2(\pm 1.1) \times 10^{-9}$ M). Note that CrmA has a large range of inhibition rate constants. Values for p35 are compared to demonstrate the relative nonspecificity of p35 for individual caspases, and the respective K_i values are upper limits (see text).

The Origin of the Strong and Specific Inhibition of Caspases by p35. The potent and highly selective inhibition of the caspases by this baculovirus protein has been extremely interesting, yet the inhibition mechanism is still poorly understood. It is now clear that p35 specifically inhibits all the caspases examined so far. Some selectivity among the caspases is achieved by p35 since K_i and k_{ass} values range by as much as 500-fold (see Table 1). However, this degree of selectivity is substantially lower than the other well-characterized natural caspase inhibitor CrmA, where K_i and k_{ass} values range over 5 orders of magnitude (*6*) (Figure 7). Moreover, CrmA is also able to inhibit the serine proteases granzyme B and glutamyl endopeptidase (*46*, *47*). Neither of these serine proteases interacted at all with p35. How is this selectivity for caspases achieved, and at the same time why is there very little discrimination between individual caspases?

The first structural determinant one would consider is the loop region, namely the residues around the cleavage site.

For example, p35 can but CrmA cannot inhibit Ced-3 in *C. elegans*. When the loop in CrmA (LVADCAST) was replaced by that of p35 (DQMDGFHD), Ced-3 was inhibited (*13*). Another report showed that mutation of Asp84 at P_4, which was not required for the cleavage at P_1 Asp87 by caspases, abolished the anti-apoptotic activity of p35 (*43*). Thus, change in the loop may confer or abolish inhibitory activities or specificities by changing the interactions between the loop and the active-site of caspases. Indeed, the three-dimensional structures of caspase-1 and -3 demonstrated that although they share a common fold, the S_4 pockets, among other things, are distinct (*41*, *48*, *49*), accounting for their substrate specificity and probably their different affinities for CrmA.

If the putative loop region of p35 contributed significantly to the specificity, it could be hypothesized that if we replace it with residues of the loop of CrmA, the mutant probably will discriminate between individual caspases as CrmA does. Furthermore, since CrmA is also an inhibitor of granzyme B, the mutant p35 might acquire inhibitory activity for granzyme B. We tested this hypothesis by replacing the P_4, P_3, P_2, and P_2' residues, which are presumably the most important non-P_1 residues in determining the specificity. Additional replacements were avoided since they might cause disruption of the loop and adjacent regions. Since the structure of p35 is unknown and no homologues of it have been found, this was a reasonable starting point for probing the structure−function relationship.

The results are indeed consistent with the prediction that the inhibitory loop would confer certain degrees of discrimination between various caspases, though the selectivity is not as prominent as CrmA. The biggest change in the standard free energy of association, seen with caspase-3, is only about 10% (∼2 kcal/mol). Thus, interactions beyond the few residues around the scissile bond may have a significant contribution to the overall potency and the selectivity. The loop mutant also turned into a substrate for granzyme B but did not become an inhibitor, further suggesting the importance of the intrinsic conformation of the inhibitory loop, or secondary sites outside of the loop region.

Comparison with Other Protease Inhibitors. A comparison of the relative strength and specificity of p35 and CrmA is shown in Figure 7. There is no homology between p35 and CrmA. Yet, there are reasons to expect that their inhibitory mechanisms may share some common features. Both proteins inhibit caspases. Unlike most other protease inhibitor families, both may be cleaved at some stage during inhibition. This property is characteristic of mechanism-based inhibitors; indeed, the serpins, of which CrmA is a member, are sometimes classified as such (*45*, *46*). Cleavage of p35 has been concluded to be necessary and sufficient for inhibition of caspases, based on the co-purification of caspase-1 and p35 cleavage products (*16*). However, one cannot rule out that cleavage is a post-denaturation event as a consequence of the attack of a well-poised nucleophile, and that the scissile bond remains intact in the native complex. For example, though a covalent bond between the scissile bond of bovine pancreatic trypsin inhibitor and trypsin was originally concluded to stabilize the complex (*50*), later crystal refinements demonstrated that this complex was a more-or-less lock-and-key interaction with minimal distortion of the scissile bond (*51*). Neither the standard mechanism inhibitors of serine proteases, such as bovine pancreatic trypsin inhibitor, nor the cystatins, which inhibit cysteine proteases of the papain family, require cleavage of the scissile bond during inhibition (*52*). Thus, the apparent cleavage of CrmA or p35 by caspases during inhibition is unusual, and future structural determinations of the p35 and CrmA complex with caspases will help to resolve the relationship between cleavage and the inhibitory mechanism.

The distinction, however, between these two caspase inhibitors is also conspicuous. For example, while CrmA is not recognized by caspase-7 (*6*), both the wild-type and the loop mutant of p35 inhibited caspase-7 with slightly different potency. The specific inhibition for caspase family and relative nondiscrimination between individual caspases by p35 is striking. One hypothesis is that there may exist some fundamental structural differences between the interaction modes of these two inhibitors with the caspases. CrmA binds in a mode which is only strong enough for some caspases, whereas p35 may have been extremely well adapted to a contact surface common to all caspases. This may involve the presence of an exosite on p35, distant from the inhibitory loop, analogous to the *E. coli* protein ecotin which is adapted to inhibiting several pancreatic serine proteases (*53*) through both primary substrate site, and distant secondary site interactions.

Biological Significance. Since the discovery of their anti-apoptotic activities, both p35 and CrmA have been extensively used as tools in dissecting the apoptosis program. Proper interpretation of these experimental results requires careful elucidation of the specificity of these viral inhibitors. We demonstrated previously that the most probable target for CrmA, among the caspases involved in Fas-mediated apoptosis, is the initiator caspase-8 (*6*). This specificity is consistent with the results of numerous studies that have shown CrmA is effective in preventing apoptosis triggered by some, but not all death stimuli (for a review, see ref *5*). The potent and highly selective inhibition by p35 of all caspases that have been tested explains its universal effectiveness in blocking apoptosis in almost all scenarios thus far reported. This also supports the notion that caspases constitute a central component of the "death machine", and hence, makes p35 an excellent reagent in establishing the involvement of caspases in apoptosis. At the same time, the lack of significant discrimination between individual caspases makes it difficult to use p35 to dissect the presumable caspase cascade composed of initiators and executioners.

Many homologues of CrmA, the serpins, are present in host genomes, though none of them seems to target caspases. Therefore it is likely that CrmA was incorporated into the poxvirus genome from a homologous host gene, and then adapted by mutation to serve a role in evading host defenses by acquiring caspase-inhibitory activity. Significantly, no homologues of p35 have been reported in animals, and the evolutionary origin of this protein is a puzzle. One would expect p35 to have been incorporated into the baculovirus genome from a homologous host progenitor, and so one of the more interesting aspects of future research on p35 will be to find a homologue in insect genomes. Is it present, and if so, is it a caspase inhibitor that regulates endogenous apoptotic pathways, or has the ancestral p35 frame been usurped from another role to inhibit caspases?

ACKNOWLEDGMENT

We thank Paul Friesen for providing the p35 cDNA, Chris Froelich for granzyme B, Martin Rechsteiner for proteasome, Nancy Thornberry for caspase-1, and Henning Stennicke and Ed Madison for helpful discussions.

REFERENCES

1. Raff, M. C. (1992) *Nature 356*, 397−400.
2. Thompson, C. B. (1995) *Science 267*, 1456−1462.
3. Nicholson, D. W., and Thornberry, N. A. (1997) *Trends Biochem. Sci. 22*, 299−306.
4. Cohen, G. M. (1997) *Biochem. J. 326*, 1−16.
5. Salvesen, G. S., and Dixit, V. M. (1997) *Cell 91*, 443−446.
6. Zhou, Q., Snipas, S., Orth, K., Dixit, V. M., and Salvesen, G. S. (1997) *J. Biol. Chem. 273*, 7797−7800.
7. Muzio, M., Chinnaiyan, A. M., Kischkel, F. C., O'Rourke, K., Shevchenko, A., Ni, J., Scaffidi, C., Bretz, J. D., Zhang, M., Gentz, R., Mann, M., Krammer, P. H., Peter, M. E., and Dixit, V. M. (1996) *Cell 85*, 817−827.
8. Clem, R. J., Fechheimer, M., and Miller, L. K. (1991) *Science 254*, 1388−1390.
9. Clem, R. J., and Miller, L. K. (1994) *Mol. Cell. Biol. 14*, 5212−5222.
10. Crook, N. E., Clem, R. J., and Miller, L. K. (1993) *J. Virol. 67*, 2168−2174.
11. Hay, B. A., Wolff, T., and Rubin, G. M. (1994) *Development 120*, 2121−2129.
12. Rabizadeh, S., LaCount, D. J., Friesen, P. D., and Bredesen, D. E. (1993) *J. Neurochem. 61*, 2318−2321.
13. Xue, D., and Horvitz, H. R. (1995) *Nature 377*, 248−251.
14. Beidler, D. R., Tewari, M., Friesen, P. D., Poirier, G., and Dixit, V. M. (1995) *J. Biol. Chem. 270*, 16526−16528.
15. Davidson, F. F., and Steller, H. (1998) *Nature 391*, 587−591.
16. Bump, N. J., Hackett, M., Hugunin, M., Seshagiri, S., Brady, K., Chen, P., Ferenz, C., Franklin, S., Ghayur, T., Li, P., et al. (1995) *Science 269*, 1885−1888.
17. Ahmad, M., Srinivasula, S., Wang, L., Litwack, G., Fernandes-Alnemri, T., and Alnemri, E. S. (1997) *J. Biol. Chem. 272*, 1421−1424.
18. Kojima, H., and Datta, R. (1996) *Oncol. Res. 8*, 497−501.
19. Datta, R., Banach, D., Kojima, H., Talanian, R. V., Alnemri, E. S., Wong, W. W., and Kufe, D. W. (1996) *Blood 88*, 1936−1943.
20. Datta, R., Kojima, H., Banach, D., Bump, N. J., Talanian, R. V., Alnemri, E. S., Weichselbaum, R. R., Wong, W. W., and Kufe, D. W. (1997) *J. Biol. Chem. 272*, 1965−1969.
21. Robertson, N. M., Zangrilli, J., Fernandes-Alnemri, T., Friesen, P. D., Litwack, G., and Alnemri, E. S. (1997) *Cancer Res. 57*, 43−47.
22. McCarthy, M. J., Rubin, L. L., and Philpott, K. L. (1997) *J. Cell Sci. 110*, 2165−2173.
23. Qi, X. M., He, H., Zhong, H., and Distelhorst, C. W. (1997) *Oncogene 15*, 1207−1212.
24. Haviv, R., Lindenboi, L., Li, H., Yuan, J., and Stein, R. (1997) *J. Neurosci. Res. 50x*, 69−80.
25. Martin, D. A., Siegel, R. M., Zheng, L., and Lenardo, M. J. (1998) *J. Biol. Chem. 273*, 4345−4349.
26. Froelich, C. J., Dixit, V. M., and Yang, X. (1998) *Immunol. Today 19*, 30−36.
27. Sorimachi, H., Ishiura, S., and Suzuki, K. (1997) *Biochem. J. 328*, 721−732.
28. Grimm, L. M., Goldberg, A. L., Poirier, G. G., Schwartz, L. M., and Osborne, B. A. (1996) *EMBO J. 15*, 3835−3844.
29. Sadoul, R., Fernandez, P. A., Quiquerez, A. L., Martinou, I., Maki, M., Schroter, M., Becherer, J. D., Irmler, M., Tschopp, J., and Martinou, J. C. (1996) *EMBO J. 15*, 3845−3852.
30. Kobayashi, T., Shinozaki, A., Momoi, T., Arahata, K., and Tsukahara, T. (1996) *J. Biochem. (Tokyo) 120* (4), 699−704.
31. Cui, H., Matsui, K., Omura, S., Schauer, S. L., Matulka, R. A., Sonenshein, G. E., and Ju, S. T. (1997) *Proc. Natl. Acad. Sci. U.S.A. 94*, 7515−7520.
32. Meriin, A. B., Gabai, V. L., Yaglom, J., Shifrin, V. I., and Sherman, M. Y. (1998) *J. Biol. Chem. 273*, 6373−6379.
33. Srinivasula, S. M., Ahmad, M., Fernandes-Alnemri, T., Litwack, G., and Alnemri, E. S. (1996) *Proc. Natl. Acad. Sci. U.S.A. 93*, 14486−14491.
34. Orth, K., O'Rourke, K., Salvesen, G. S., and Dixit, V. M. (1996) *J. Biol. Chem. 271*, 20977−20980.
35. Muzio, M., Salvesen, G. S., and Dixit, V. M. (1997) *J. Biol. Chem. 272*, 2952−2956.
36. Komiyama, T., Gron, H., Pemberton, P. A., and Salvesen, G. S. (1996) *Protein Sci. 5*, 874−882.
37. Baugh, R., and Travis, J. (1976) *Biochemistry 15*, 836−841.
38. Bury, A. (1981) *J. Chromatogr. 213*, 491−500.
39. Matsudaira, P. (1987) *J. Biol. Chem. 262*, 10035−10038.
40. Morrison, J. F., and Walsh, C. T. (1988) *Adv. Enzymol. Relat. Areas Mol. Biol. 59*, 201−301.
41. Rotonda, J., Nicholson, D. W., Fazil, K. M., Gallant, M., Gareau, Y., Labelle, M., Peterson, E. P., Rasper, D. M., Tuel, R., Vaillancourt, J. P., Thornberry, N. A., and Becher, J. W. (1996) *Nat. Struct. Biol. 3*, 619−625.
42. Mittl, P. R., Di Marco, S., Krebs, J. F., Bai, X., Karanewsky, D. S., Priestle, J. P., Tomaselli, K. J., and Grutter, M. G. (1997) *J. Biol. Chem. 272*, 6539−6547.
43. Bertin, J., Mendrysa, S. M., LaCount, D. J., Gaur, S., Krebs, J. F., Armstrong, R. C., Tomaselli, K. J., and Friesen, P. D. (1996) *J. Virol. 70*, 6251−6259.
44. Barrett, A. J., Kembhavi, A. A., Brown, M. A., Kirschke, H., Knight, C. G., Tamai, M., and Hanada, K. (1982) *Biochem. J. 201*, 189−198.
45. Patston, P. A., Gettins, P. G. W., and Schapira, M. (1994) *Ann. N.Y. Acad. Sci. 714*, 13−20.
46. Komiyama, T., Ray, C. A., Pickup, D. J., Howard, A. D., Thornberry, N. A., Peterson, E. P., and Salvesen, G. (1994) *J. Biol. Chem. 269*, 19331−19337.
47. Komiyama, T., Quan, L. T., and Salvesen, G. S. (1995) in *Intracellular Protein Catabolism* (Suzuki, K., and Bond, J. S., Eds.), pp 173−176, Plenum Press, New York.
48. Wilson, K. P., Black, J. A., Thomson, J. A., Kim, E. E., Griffith, J. P., Navia, M. A., Murcko, M. A., Chambers, S. P., Aldape, R. A., Raybuck, S. A., and Livingston, D. J. (1994) *Nature 370*, 270−275.
49. Walker, N. P. C., Talanian, R. V., Brady, K. D., Dang, L. C., Bump, N. J., Ferenz, C. R., Franklin, S., Ghayur, T., Hackett, M. C., Hammill, L. D., Herzog, L., Hugunin, M., Houy, W., Mankovich, J. A., McGuiness, L., Orlewicz, E., Paskind, M., Pratt, C. A., Reis, P., Summani, A., Terranova, M., Welch, J. P., Xiong, L., and Möller, A. (1994) *Cell 78*, 343−352.
50. Rühlmann, A., Kukla, D., Schwager, P., Bartels, K., and Huber, R. (1973) *J. Mol. Biol. 77*, 417−436.
51. Huber, R., Bode, W., Kukla, D., and Kohl, U. (1975) *Biophys. Struct. Mech. 1*, 189−201.
52. Bode, W., and Huber, R. (1992) *Eur. J. Biochem. 204*, 433−451.
53. McGrath, M. E., Erpel, T., Bystroff, C., and Fletterick, R. J. (1994) *EMBO J. 13*, 1502−1507.

BI980893W